REPORT DOCUMENTATION PAGE

Form Approved
OMB No. 0704-0188

Public reporting burden for this collection of information is estimated to average 1 hour per response, including the time for reviewing instructions, searching existing data sources, gathering and maintaining the data needed, and completing and reviewing this collection of information. Send comments regarding this burden estimate or any other aspect of this collection of information, including suggestions for reducing this burden to Department of Defense, Washington Headquarters Services, Directorate for Information Operations and Reports (0704-0188), 1215 Jefferson Davis Highway, Suite 1204, Arlington, VA 22202-4302. Respondents should be aware that notwithstanding any other provision of law, no person shall be subject to any penalty for failing to comply with a collection of information if it does not display a currently valid OMB control number. **PLEASE DO NOT RETURN YOUR FORM TO THE ABOVE ADDRESS.**

1. REPORT DATE *(DD-MM-YYYY)*	**2. REPORT TYPE**	**3. DATES COVERED** *(From - To)*
January 2015	Technical Paper	January 2015- May 2015

4. TITLE AND SUBTITLE
High Heat Flux Surface Coke Deposition and Removal Assessment

5a. CONTRACT NUMBER
FA9300-13-C-2012

5b. GRANT NUMBER

5c. PROGRAM ELEMENT NUMBER

6. AUTHOR(S)

Wickham, D., J. Engel, B. Hitch, A. Wickham

5d. PROJECT NUMBER

5e. TASK NUMBER

5f. WORK UNIT NUMBER
Q0A5

7. PERFORMING ORGANIZATION NAME(S) AND ADDRESS(ES)

Air Force Research Laboratory (AFMC)
AFRL/RQRC
10 E. Saturn Blvd
Edwards AFB CA 93524-7680

8. PERFORMING ORGANIZATION REPORT NO.

9. SPONSORING / MONITORING AGENCY NAME(S) AND ADDRESS(ES)
Air Force Research Laboratory (AFMC)
AFRL/RQR
5 Pollux Drive
Edwards AFB CA 93524-7048

10. SPONSOR/MONITOR'S ACRONYM(S)

11. SPONSOR/MONITOR'S REPORT NUMBER(S)
AFRL-RQ-ED-TP-2015-281

12. DISTRIBUTION / AVAILABILITY STATEMENT
Distribution A: Approved for public Release; distribution unlimited

13. SUPPLEMENTARY NOTES
Technical paper presented at the AIAA Propulsion and Energy Forum and Exposition (Joint Propulsion Conference)in Orlando, FL; 27-29 July, 2015

14. ABSTRACT

The internal surfaces of liquid hydrocarbon-fueled rocket engine thrust chambers, throats, and nozzles are exposed to high pressure combustion products at temperatures beyond 6000 F. Regenerative cooling is widely used in these engines to prevent overheating of the copper alloy liners. As a result, high heat flux fuel-wetted surfaces reach temperatures where fuel carbon deposits (coke) form. Coke has a much lower thermal conductivity than copper - thicknesses of only a few millionths of an inch can cause liner temperatures to increase to dangerous levels. Moreover, reusing launch vehicles and main engines increases the likelihood that unsafe levels of coke will be deposited over the course of multiple missions. Therefore, there is a need for a method to survey coke layer thicknesses and locations in the cooling channels so that engine operating margins, service intervals, and lifetimes can be determined. Unfortunately, the cooling channel geometry combined with thin coke layers makes this a difficult and challenging problem. Reaction Systems, Inc. has developed a low temperature oxidation method that can rapidly remove the coke layers in the cooling channels and at the same time map their location. We demonstrated this technique in a recent SBIR Phase II effort, which included depositing coke on copper surfaces at heat fluxes in excess of 20 Btu/in2-s under pressure, temperature, and flow conditions that match those experienced in liquid hydrocarbon-fueled rocket engines. Surface analysis was used to characterize the carbon concentration on the surface of the copper substrate after the coking cycle and also measure the thickness of the carbon deposit. These analyses were used to also demonstrate that the carbon was completely removed from the substrate using our low temperature oxidation process. Finally, the surface analyses indicated that a substantial copper sulfide layer had accumulated on the substrate after the coking cycle even with the low sulfur concentrations in RP-2. This material was also removed or at least reduced with our low temperature oxidation process.

15. SUBJECT TERMS

16. SECURITY CLASSIFICATION OF:			**17. LIMITATION OF ABSTRACT**	**18. NUMBER OF PAGES**	**19a. NAME OF RESPONSIBLE PERSON**
					Matt Billingsley
a. REPORT	**b. ABSTRACT**	**c. THIS PAGE**	SAR	21	**19b. TELEPHONE NO** *(include area code)*
Unclassified	**Unclassified**	**Unclassified**			661-275-5885

Standard Form 298 (Rev. 8-98)
Prescribed by ANSI Std. 239.18

High Heat Flux Surface Coke Deposition and Removal Assessment

David T. Wickham[1], Jeffrey R. Engel[2], Bradley D. Hitch[3], and Alex R. Wickham[4]
Reaction Systems, Inc., Golden, CO 80401

The internal surfaces of liquid hydrocarbon-fueled rocket engine thrust chambers, throats, and nozzles are exposed to high pressure combustion products at temperatures beyond 6000°F. Regenerative cooling is widely used in these engines to prevent overheating of the copper alloy liners. As a result, high heat flux fuel-wetted surfaces reach temperatures where fuel carbon deposits (coke) form. Coke has a much lower thermal conductivity than copper - thicknesses of only a few millionths of an inch can cause liner temperatures to increase to dangerous levels. Moreover, reusing launch vehicles and main engines increases the likelihood that unsafe levels of coke will be deposited over the course of multiple missions. Therefore, there is a need for a method to survey coke layer thicknesses and locations in the cooling channels so that engine operating margins, service intervals, and lifetimes can be determined. Unfortunately, the cooling channel geometry combined with thin coke layers makes this a difficult and challenging problem. Reaction Systems, Inc. has developed a low temperature oxidation method that can rapidly remove the coke layers in the cooling channels and at the same time map their location. We demonstrated this technique in a recent SBIR Phase II effort, which included depositing coke on copper surfaces at heat fluxes in excess of 20 Btu/in2-s under pressure, temperature, and flow conditions that match those experienced in liquid hydrocarbon-fueled rocket engines. Surface analysis was used to characterize the carbon concentration on the surface of the copper substrate after the coking cycle and also measure the thickness of the carbon deposit. These analyses were used to also demonstrate that the carbon was completely removed from the substrate using our low temperature oxidation process. Finally, the surface analyses indicated that a substantial copper sulfide layer had accumulated on the substrate after the coking cycle even with the low sulfur concentrations in RP-2. This material was also removed or at least reduced with our low temperature oxidation process.

Nomenclature

h	=	heat transfer coefficient (W/m^2-°K)
k	=	thermal conductivity (W/m-K)
q''	=	heat flux (Btu/in^2-s or W/m^2)
R	=	radius
Re	=	Reynolds number
T	=	temperature (°C)
δ	=	thermal boundary layer thickness

I. Introduction

Rocket engines rely on high pressure combustion to generate thrust by expelling hot gas out of a nozzle at high velocity. The internal surfaces of the thrust chamber, throat, and nozzle must be able to withstand contact with the high pressure combustion products at temperatures beyond 6000°F. Moreover, the drive to increase engine thrust to weight ratio is pushing thrust chamber pressures and heat fluxes to higher values, placing additional demand on

[1] President, 17301 W. Colfax Avenue, Suite 160, Senior Member AIAA.
[2] Chief Operating Officer, 17301 W. Colfax Avenue, Suite 160, Senior Member AIAA.
[3] Chief Engineer, 17301 W. Colfax Avenue, Suite 160, Senior Member AIAA.
[4] Engineer, 17301 W. Colfax Avenue, Suite 160.

Distribution A: Approved For Public Release. Unlimited Distribution.

the systems that cool these surfaces[1]. For example, increasing the chamber pressure from 70 atm in the Saturn V F-1 engine to 250 atm in the RD-180 (the current state of the art in LOx/kerosene engines) increases the gas-side throat heat flux from 10 to 70 Btu/in^2-s. Throat gas-side heat fluxes of up to 100 Btu/in^2-s are considered possible in future high performance LOx/kerosene engines.

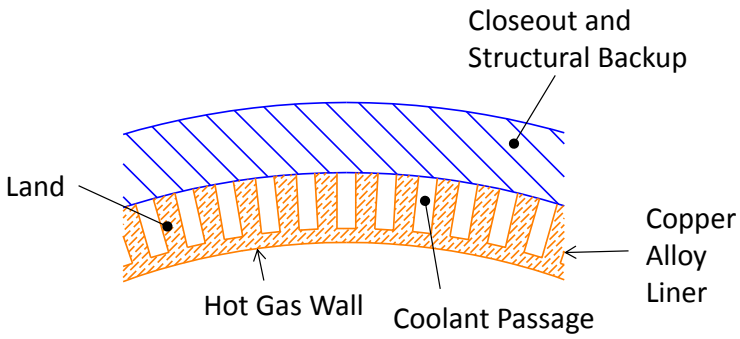

Figure 1. Rocket engine liner cooling channels[2].

Although there are a number of methods available to cool rocket engine thrust chambers and nozzle walls sufficiently, regenerative cooling, where fuel is fed though passages in the thrust chamber walls on the way to the combustor, is widely used in liquid-fueled rocket engines (Figure 1). Perhaps the greatest advantages of regenerative cooling over other methods are 1) the engine geometry and performance is nearly unaffected by engine operating time and 2) there is essentially no loss of heat from the system; all of the thermal energy absorbed by the fuel is subsequently delivered to the combustion process.

There are some disadvantages of regenerative cooling, however. These include high gas-side surface heat fluxes resulting from the limited temperature capability and strength of available high thermal conductivity materials. While some relief can be obtained by expansion in the effective fuel-side to gas-side surface area through fin conduction, narrow passages and high fuel velocities must be used to obtain the high fuel-side heat transfer coefficients required to maintain liner structural integrity. This results in significant fuel-side pressure drops and increased fuel pumping power. Fuel-side heat transfer surfaces are therefore designed to operate as hot as possible to minimize this pressure loss. Consequently, fuel-side heat transfer surfaces commonly operate at temperatures where carbon deposits (coke) can form, ca. 750 to 950°F (~400 to 500°C). As illustrated in Figure 2, the accumulation of coke layers on the fuel side increase the overall thermal resistance of the liner and cause the copper wall temperatures to rise.

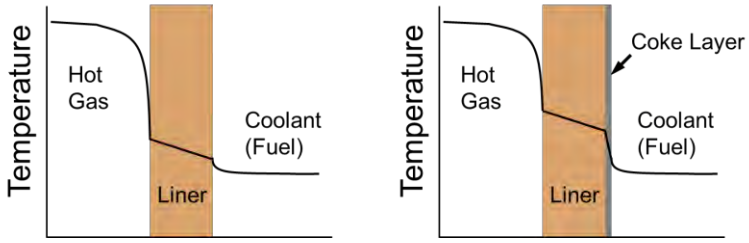

Figure 2. Engine liner temperature distribution: left side no coke accumulation; right side; with coke accumulation.

A. Effect of Fuel-Side Coke on Rocket Engine Liner Temperatures

Figure 3 shows the liner temperature rise as a function of the coke layer thickness and fuel-side surface heat flux for heat fluxes from 5 to 50 Btu/in^2-sec, assuming an effective coke thermal conductivity of 0.07 Btu/ft-hr-R. This value for the coke thermal conductivity lies within the ranges reported by Hazlett[3] and is approximately 3000 times lower than the conductivity of OFHC copper at 500°C (932°F). Assuming a factor of two increase in effective heat transfer surface area from the hot gas to fuel-side means that the fuel-side heat flux corresponds to roughly half that of the hot gas surface. For instance, the line denoted 5 Btu/in^2-s corresponds to a gas-side heat flux of about 10 Btu/in^2-s, while the 50 Btu/in^2-s line corresponds to a 100 Btu/in^2-s gas-side heat flux. Figure 3 indicates that a fuel-side coke layer of only about 2 millionths of an inch would cause a 60°F rise in the liner temperature with a fuel side heat flux of 50 Btu/in^2-sec, while a coke layer ten times thicker or 20 millionths of an inches could produce the same liner temperature rise with a gas-side heat flux of only 10 Btu/in^2-sec. This result indicates that the thicknesses of thermally significant coke layers are on the order of the wavelength of ultraviolet light, making them impossible to quantify with normal optical microscopic techniques.

Although current engines are designed to tolerate the quantities of coke that are typically deposited in a single mission, there is now a strong interest in reusing liquid-fueled rocket engines to reduce costs. This raises new questions regarding the number of missions an engine can complete without accumulating dangerous levels of coke. Therefore, there is now a strong need to characterize coke layers that accumulate under high heat flux conditions and identify effective methods to remove these layers between missions.

Distribution A: Approved For Public Release. Unlimited Distribution.

B. A Method to Assess and Remove Engine Coke Deposits

In a previous paper[4] we described a patent-pending approach to simultaneously map and remove coke deposited in all of the cooling channels in a rocket engine in a short period of time. This method can provide coke deposit thickness and location information that can be used to set service intervals and predict lifetimes from development hydrocarbon-fueled engines, as well as to clean reusable flight engines. It is fast, safe, and creates no potential to leave any hardware in the channels while completely removing all carbon deposits, eliminating the need for additional maintenance or downtime. We described the results obtained in a recently completed SBIR Phase I project which demonstrated that the location and thickness of coke layers deposited in copper test sections could be determined by monitoring the outer surface temperature of a test article with a thermal imaging camera while the coke inside the test section was oxidized at low temperature to CO_2 using a dilute flow of ozone. We also showed that the oxidation of a coke layer that is only one millionth of an inch thick should result in a temperature rise of ~1°C, which can be detected by commercially available LWIR thermal imaging cameras. Finally, the overall quantity of coke can be measured by monitoring the CO_2 concentration in the effluent during the oxidation process.

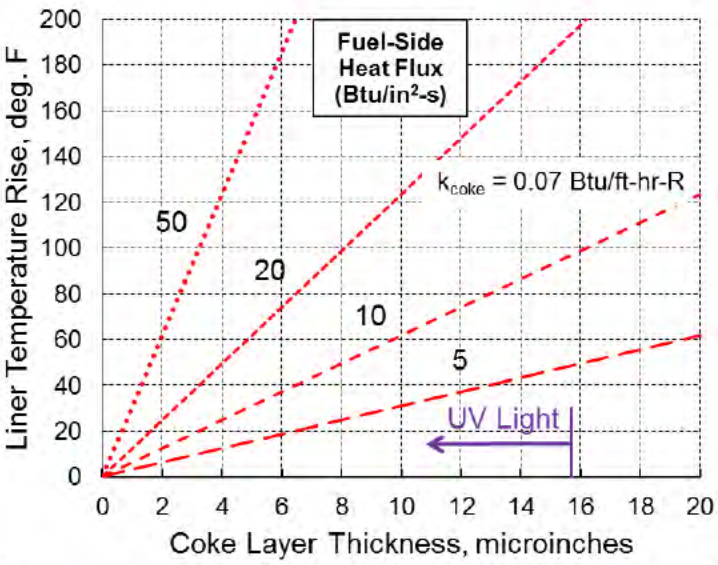

Figure 3. Liner temperature rise versus coke layer thickness for various levels of fuel-side surface heat flux.

As a result we created a conceptual design of a thermal imaging system using a moving conical mirror that would allow us to obtain thermal images of the internal surfaces of a rocket engine during the decoking process, as shown in Figure 4. We also designed a rapid heating procedure using both an external electrically-heated blanket and a combustion-fired convective heater that could bring the engine up to temperature and hold it there for the duration of the decoking and coke mapping process. We estimated that the total time required to decoke an engine using this process would be on the order of 1 hour.

C. Oxidation of Rocket Engine Coke Deposits

The results that we obtained in the SBIR Phase I project were quite promising but were not obtained with real coke deposited under high heat flux conditions. Moreover, one of the difficulties in the study of coke deposition is understanding the effects that variables such as temperature, pressure, heat flux, velocity etc. have on coolant-side coke formation mechanisms and the resulting coke morphology. One important variable that is difficult to simulate in the laboratory is heat flux. Edwards[1] discusses the effect that very thin coke layers have on heat transfer in rocket engine cooling channels and cites a value of 0.07 Btu/ft-hr-°F for the thermal conductivity of coke.

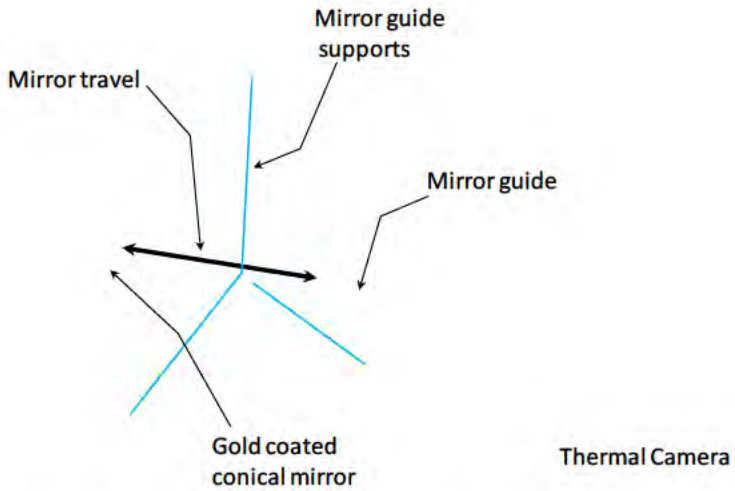

Figure 4. Conceptual design of a translating mirror system to allow optical access to the engine interior.

Distribution A: Approved For Public Release. Unlimited Distribution.

Unfortunately, this value was obtained for carbon deposited under aircraft fuel system conditions, not those expected in a rocket engine and there is significant uncertainty associated with this value. For example, Hazlett[3] cites values ranging from 0.022 to 0.12 Btu/ft-hr-°F. Therefore, understanding the effects that heat flux and other parameters such as pressure, fuel flow velocity, temperature, etc. have on coke deposition from RP-1 and RP-2 as well as showing that we can oxidize and remove these deposits using ozone, would be very valuable in the development of new rocket engines and in particular those that will be reused.

II. Previous High Heat Flux Coke Deposition Research

Several experiments investigating coke deposition from hydrocarbon fuels under high pressure, high flow velocity and high heat flux conditions have been reported in the literature. Roback et al.[5] conducted experiments with RP-1, JP-7 and propane at heat fluxes up to 8.9 Btu/in^2-s. Rosenburg and Gage[6] reported studies with RP-1 and *n*-dodecane. They conducted tests at pressures up to 3500 psig, with maximum wall temperatures of 293°C to 427°C (560-800°F) at the reactor exit, and achieved heat fluxes up to 20 Btu/in^2-s. The results of this work led to the conclusion that the dominant copper corrosion mechanism was the formation of copper sulfide and that sulfur levels in the fuel as low as 1 ppm can cause rapid corrosion and significantly affect the performance of the cooling channels. They also determined that the effects of sulfur could be eliminated by plating the channels with gold. Billingsley[7] conducted tests focused on characterizing the thermal stability of RP-2 under high heat flux conditions. Sulfur levels in RP-2 are less than 0.1 ppm, and therefore work conducted with RP-2 fuel is less likely to be affected by the formation of copper sulfide. Tests were carried out in the High Heat Flux Facility at Edwards AFB, which produced wetted wall temperatures up to 885°F, heat fluxes from 6.1 to 7.3 Btu/in^2-s, inlet fuel velocities ranging from 50 to 75 ft/s, and inlet Reynolds from 11,300 to 34,300. A LECO carbon analyzer was used to characterize coke deposition within the tubes after testing. Measurable coke deposition was obtained in all runs but lower values were observed in the first two tests. It was concluded that the reduced deposition in the first two tests, which used unstressed fuel, could have been due to lower concentration of precursors in the bulk fuel. Van Noord et al.[8] carried out tests in copper tubes at pressures up to 1000 psi, with heat fluxes up to 6 Btu/in^2-s and with wall temperatures that reached 637°C (1180°F). At wall temperatures greater than 454°C (850°F) they found that measured wall temperatures along the length of the tube began to rise and then drop rapidly. This behavior was attributed to the cyclic build-up of carbon layers on the wall followed by rapid shedding of the coke layer. Kleinhenz et al.[9] also reported tests in the heated tube facility at NASA Glenn Research Center using resistively heated copper tubes and RP-2. Wall temperatures were in the range of 454°C to 565°C (850-1050°F), the fuel velocity was 75 ft/s, the pressure was held constant at 1000 psia and heat fluxes up to 5.98 Btu/in^2-s. Tests were conducted on different batches of RP-2 and the effect of an additive, 1,2,3,4-tetrahydroquinoline (THQ) was observed. Coke deposits ranged from about 10 μg/cm^2 up to 70 μg/cm^2 and the presence of THQ appeared to increase the rate of coke deposition.

Studies have also been conducted to characterize heat transfer characteristics under high heat flux conditions. For example, Billingsley et al.[10] conducted studies with RP-2 at high heat flux conditions in order to extract heat transfer coefficients. The sulfur levels in the fuel were less than 0.1 ppm and tests were carried out at pressures from 85 to 1735 psig, with wall temperatures at the exit on the order of 450°C to 610°C (840 - 1130°F) and bulk fuel temperatures up to 160°F. Heat fluxes were between 2 to 10 Btu/in^2-s, with fuel velocities of 26 to 165 ft/s and Reynold's numbers that ranged from 5500 to 33000. They developed a Nusselt number correlation that agreed to within ±20% of the data obtained under these conditions. Another study was directed at hypersonic vehicles and was done with Inconel tubes, which eliminated complications caused by interactions between even trace levels of sulfur in the fuel and copper[11]. The authors conducted tests in the heated tube facility at NASA Glenn Research Center where wall temperatures reached 900°C (1650°F) and maximum heat fluxes were 5 Btu/in^2-s. They compared Nusselt numbers measured in their work to those predicted by the classic Sieder-Tate and Dittus Boelter correlations and overall obtained the best agreement with Sieder-Tate.

While the previous work provides a good framework to carry out coke deposition measurements under relevant conditions, most of the papers described above did not include surface analyses on the copper metal in contact with the fuel, so relative concentrations of carbon, copper and sulfur were not quantified. While combustion methods are effective at measuring total carbon, they do not provide information on the concentration of contaminants as a function of depth into the substrate surface, which should be valuable in estimating the lifetime or number of cycles a rocket engine can safely provide. As described in the following section, our test rig was designed to expose a copper test section to relevant high heat flux test conditions and then be easily removed for surface analysis and depth profiling by Auger Electron Spectroscopy (AES).

Distribution A: Approved For Public Release. Unlimited Distribution.

III. Experimental Methods

The experimental apparatus and methods developed to deposit coke on a wire under high pressure, high flow velocity and high heat flux conditions in the Phase II project are presented in this section. We first describe the design of the High Heat Flux wire experiment then show details of the actual hardware constructed in the project.

A. High Heat Flux Wire Experiment - Conceptual Design

Based on a review of previous research on rocket engine cooling with hydrocarbon fuels as well as our own analysis of the likely thicknesses of relevant coke layers discussed above, we designed a high heat flux coke deposition experiment that could exactly match all of the pertinent variables, including cooled surface heat flux, bulk fuel pressure and temperature, fuel bulk velocity, channel hydraulic diameter, bulk Reynolds Number, and surface to bulk temperature ratio.

In addition, by using an electrically heated wire instead of a tube to achieve these conditions we accomplished two goals:

1) Deposit high heat flux coke on an easily accessible external surface allowing easy surface analysis.

2) Limit the scale of the experiment to minimize the cost of the equipment.

Our test section was designed to simulate the copper heat transfer surfaces in the cooling channels of a rocket engine by directing electrical current through a thin copper wire surrounded by flowing RP-2. A schematic of the system layout is shown in Figure 5. A bladder accumulator, which could be pressurized to 3000 psig, contained approximately 9 gallons of RP-2. An upstream turbine flowmeter was used to measure the liquid fuel flow rate while a Badger valve controlled the flow through the test section containing the wire, using feedback from the turbine meter. Fuel flow rates ranged from 1 gallon per minute up to 3.1 gallons per minute. Current provided by a 20 Volt - 750 Amp DC power supply was used to heat the copper wire. Wire diameters ranged from 0.005 up to 0.020 inches (0.13 to 0.50 mm). Finally, a scrap tank collected the expended fuel at the end of each test. Test durations were up to three minutes at the highest flow rates, which is similar to typical burn times of a 1st stage rocket engine. Fuel temperatures were measured going into and exiting the test section. Since the bulk fuel temperature was only increased by a maximum of about 25°C in each test, the fuel could be reused by transferring it back into the bladder accumulator if desired. In addition, we measured the voltage across the wire and used the current output signal from the power supply to monitor the delivered power during each test. The wire surface heat flux was obtained from the delivered power and the wire surface area based on the measured length and diameter of the wire. We also used the measured current and voltage to determine the wire resistance, then used the tabulated material resistivity versus temperature dependence to evaluate the wire temperature and the surface heat transfer coefficient. Heat balances were typically within 2% after the initial startup transient.

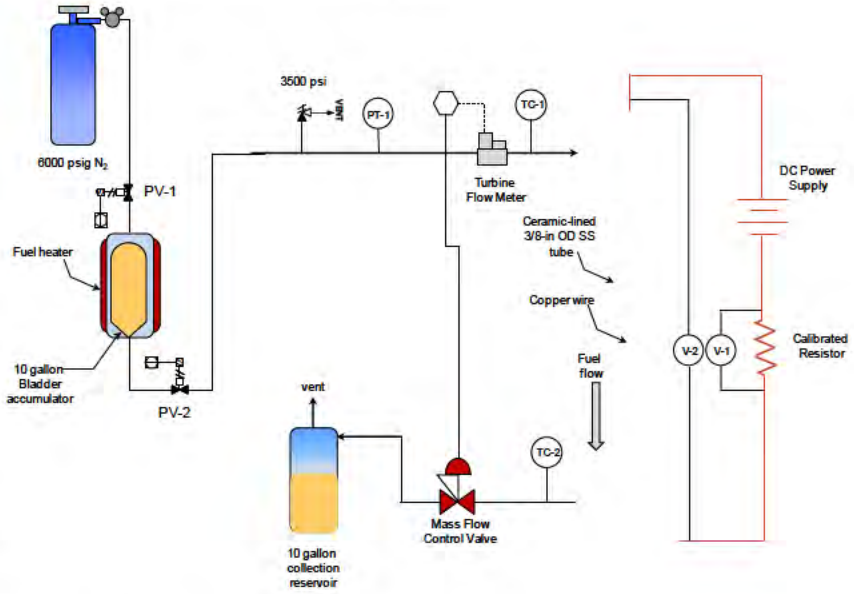

Figure 5. High Heat Flux Wire experiment conceptual design.

B. Detailed Design of the High Heat Flux Wire Experiment

The nominal rocket engine cooling passage size that we identified during the Phase I project was a rectangular channel 0.050-in wide and 0.150-in tall (3:1 aspect ratio, D_{hyd} = 0.075-in.) with 0.050-in lands between the channels and a 0.035-in thick facesheet, shown schematically above in Figure 1. Rectangular liner coolant passages allow the engine designer to keep the channel width small to minimize stresses in the face sheet while also providing additional flow area compared to round channels. These liner cooling passages are milled into the back side of the liner before assembly and brazing to the structural jacket/closeout. This configuration allows some spreading of the liner gas-side heat flux due to the fin conduction function of the lands between the channels. Even though copper is a very high thermal conductivity material, high fuel-side heat transfer coefficients limit the fin effectiveness that can be obtained. This results in approximately a factor of two larger effective heat transfer surface area on the coolant side of the liner versus the inner hot gas side.

While there is an apparent geometry difference between a rocket engine cooling passage and our hot wire experiment, the scale of the thermal boundary layer is actually more than an order of magnitude smaller than the radius of curvature of the wire surface. This means that the boundary layer temperature profile is indistinguishable from that on a flat surface even with the smallest diameter wire tested (0.13 mm or 0.005 inch).

The scale of the thermal boundary layer can be estimated by setting the heat flux at the surface of the wire equal to the conduction of heat into the fluid:

$$\dot{q}'' = -k\left.\frac{dT}{dy}\right|_s = h(T_s - T_{bulk}) \qquad -\frac{k(T_{bulk} - T_s)}{\delta_T} = h(T_s - T_{bulk}) \qquad \delta_T \approx \frac{k}{h}$$

Where k is the surface fluid thermal conductivity, *dT/dy* is the temperature gradient in the fluid next to the surface, T_s is the surface temperature, T_{bulk} is the bulk fluid temperature, δ_T is the length scale of the thermal boundary layer, and *h* is the convective heat transfer coefficient. Correlations for turbulent convective heat transfer provide the value for *h* in conjunction with the physical properties of the fluid and flow parameters like Reynolds number. By substituting the relevant parameters at the design point of our HHF Test Section, we obtain:

$$\delta_T \approx \frac{0.093\ W/m-K}{67800\ W/m^2-K} = 1.37 \times 10^{-6}\ \text{m} \quad (5.4 \times 10^{-5}\ \text{inch})$$

A wire with a diameter of 0.005 inch (0.13 mm) has a surface curvature radius of 0.0025 inch, therefore the ratio of the scale of the thermal boundary layer to the radius of curvature of the wire surface is:

$$\frac{\delta_T}{R_{wire}} = \frac{5.4\times10^{-5}}{0.0025} = 0.022 = 2.2\%$$

The thickness of the thermal boundary layer on the wire is therefore negligible compared to the curvature of the surface, meaning that the temperature distribution through the boundary layer will be nearly identical to that of a flat surface. The coking data that we collect with the wire therefore should be directly relevant to the local hot surface of a rocket engine cooling channel operating under the same fuel flow and heat flux conditions.

Distribution A: Approved For Public Release. Unlimited Distribution.

Detailed drawings of the test section we constructed in this project to simulate the flow characteristics described above are shown in Figure 6. The test section at the center of the system consists of a 3.9 inch length of 3/8-in OD 17-4PH stainless steel tube with a reduced ID where fuel flows over a 3.8 inch length of copper wire, copper ribbon, or a copper coupon. The 3/8-in OD tube was lined with a Teflon insert to insulate the wire and prevent a short circuit as well as set the ID of the test section at 0.080 inches. Small wire feedthroughs at the top and bottom are used to measure the voltage difference across the wire under test. The wire or coupon is soldered into upper and lower busbar connectors then inserted into the test section from the top after removing the upper and lower wire ΔV feedthroughs. The current needed to heat the wire is delivered with 5/16-in diameter OFHC copper busbars. These busbars penetrate into the high pressure test assembly through Conax-Buffalo feedthroughs that can seal against pressures up to 5000 psig. The lower busbar was fitted with a 1.5-in length of flexible cable designed to accommodate the thermal growth of the wire and keep it under spring tension during a test.

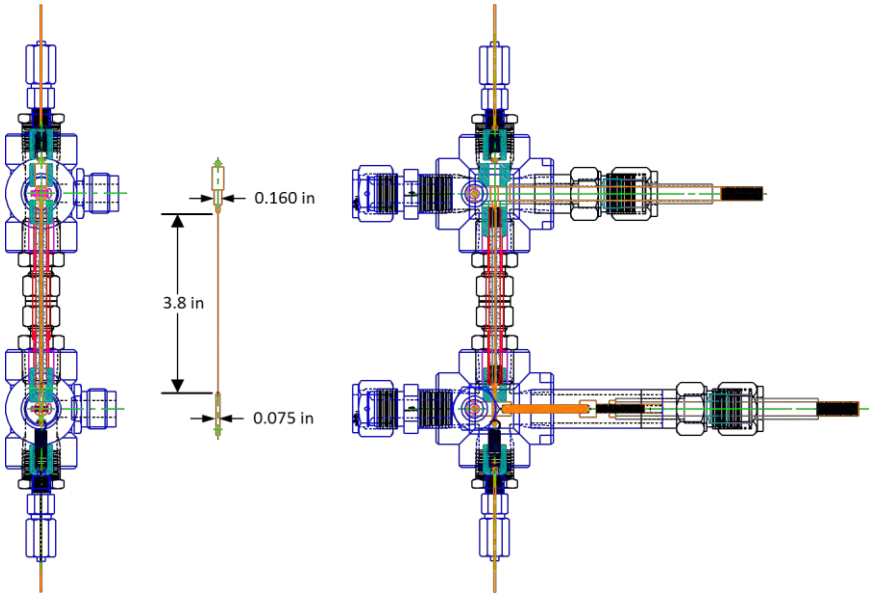

Figure 6. AutoCAD assembly drawing of the High Heat Flux test section and copper wire insert.

The diameter or cross sectional area of the wire can be adjusted to obtain the heat flux desired, with smaller cross sectional areas having increased resistance per inch and capable of higher heat flux. For example, the resistance of a 0.005-in diameter Cu wire is 0.414 ohms per foot of length and therefore for a length of 3.8 inches the total resistance is 0.131 ohms. With a current of 100 amps passing through the wire, the total power is then 1311 watts or 1.24 Btu/s. Finally, the surface area of the wire is 0.060 in^2 and therefore the heat flux from the surface of the wire to the fuel would be 20.9 Btu/in^2-s. Varying the current, wire diameter, fuel flow rate, and pressure provide flexibility in obtaining coke deposits over a wide range of surface temperatures, heat fluxes, flow velocities, and Reynolds numbers.

Distribution A: Approved For Public Release. Unlimited Distribution.

Figure 7 shows the individual components of the High Heat Flux test section before they were welded or inserted into place. The fuel flow proceeded from the left VCR port in the top fitting into the test section, shown in the center of the figure and then out the left VCR port on the left side of the lower fitting. The top and bottom crosses were machined to accept additional VCR fittings as access ports directly over the busbar clamp screws. We used UNS18200 chrome copper to fabricate the busbar clamps due to its much higher strength than the Oxygen Free Electronic (OFE) copper that was originally supplied with the feedthroughs. The wire under test was soldered into the upper and lower busbar inserts which are clamped into the busbars. The wire is held in the center of the teflon-lined test section with teflon guides that thread onto both ends of the 3/8-in OD test section, which each have four ⅛-in diameter holes to allow the fuel to flow into and out of the test section. These guides also serve to control the gap between the busbar connection and the mouth of the Teflon insert. The upper busbar insert has a ¼-in OD cylindrical plug that fits inside of the upper Teflon guide to provide the proper alignment of the upper busbar connection. As mentioned before, the power dissipated by the wire in the fuel is the product of the measured voltage and the current through the wire, which is monitored using the output signal from the DC power supply. External heat losses are minimal from this configuration.

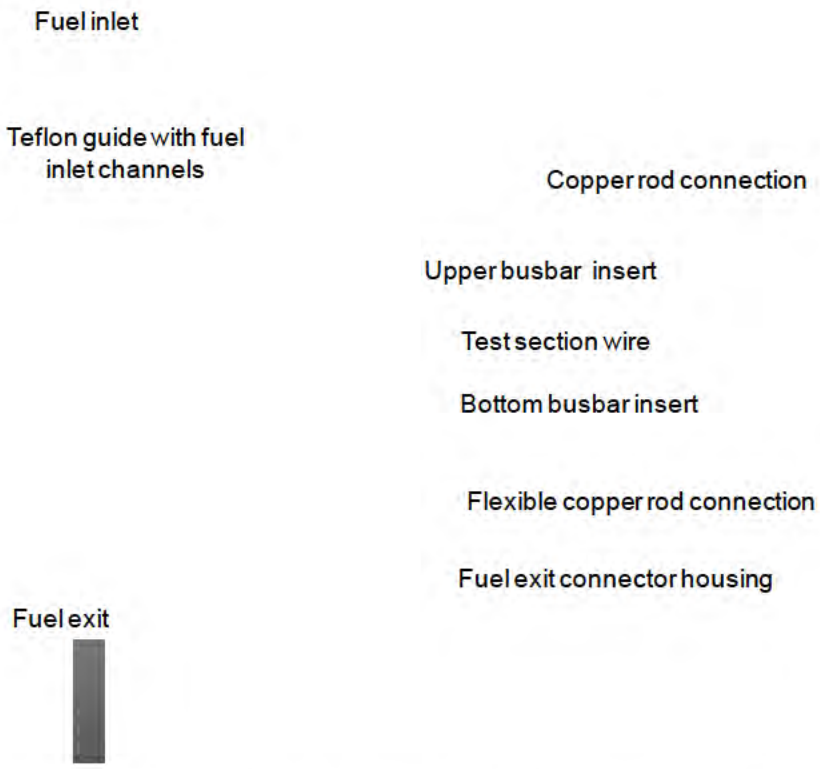

Figure 7. Photograph of the High Heat Flux test section components showing their relative size and position.

Photographs of the completed High Heat Flux test section installed on our test rig are shown in Figure 8, Figure 9, and Figure 10. Figure 8 is a close up view of the completed test section assembly. The 1/2-in OD fuel lines going into and out of the test section are

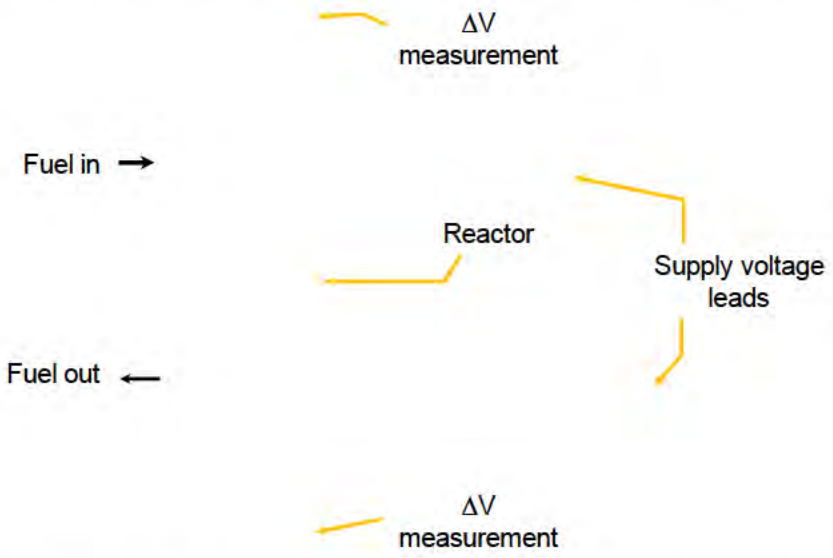

Figure 8. Close up photograph of the assembled test section mounted on the automated test rig.

visible on the left side, while the electrical feedthroughs and the leads to the DC power supply can be seen on the right. Finally, the wires coming through feedthroughs at the top and bottom of the test section that are used to monitor the differential voltage across the wire are also visible.

Figure 9 shows the test section installed on the rig along with the instrumentation and hardware needed to support its operation. The Badger flow control valve is shown to the lower right of the test section while the blue Omega turbine flow meter is visible on the left side of the test section.

Finally, Figure 10 shows a photo taken from the right side of the test rig seen in Figure 8 and Figure 9. In this view the 10 gallon accumulator used to hold and pressurize the fuel supply is seen on the left. The blue turbine flow meter is more clearly visible in this view, and finally the scrap tank is also shown on the bottom of the test rig frame. We generate the flow in this system by pressurizing the bladder accumulator and allowing the fuel to exit through the flow control valve in a single pass through the test section and then exit into the scrap tank. With the capacities of the accumulator and scrap tank, and at flow rates of up to 3.1 gal/min, we can conduct tests for periods of up to 3 minutes or more, approximating the typical burn time of a LOx/RP booster engine during launch.

IV. Results

In this section we present the results of the high heat flux tests carried out on copper wires along with copper clad stainless steel (CCS) wires, and also discuss the heat transfer

Figure 9. Photograph of the installed test section and the supporting instrumentation and hardware.

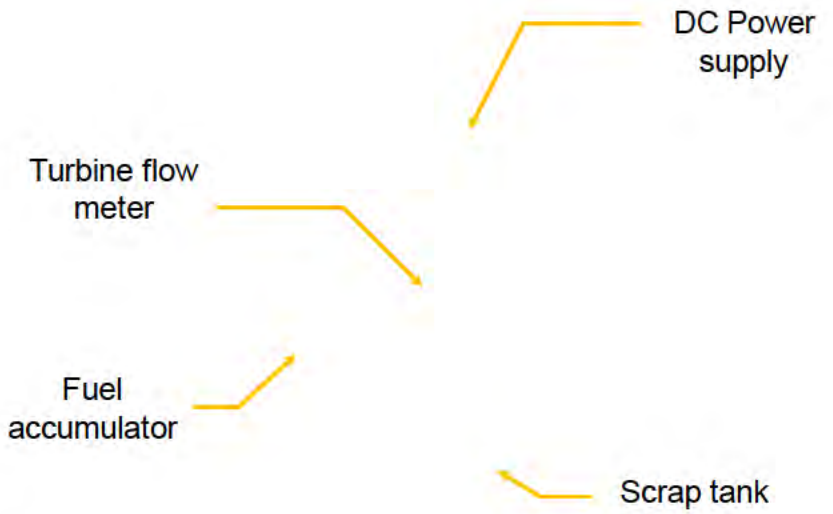

Figure 10. Side view of the test rig showing the fuel accumulator and scrap tank.

Distribution A: Approved For Public Release. Unlimited Distribution.

characteristics observed in these tests. We then present surface analyses carried out on the wires after coke deposition and also following our low temperature oxidation process.

A. Results of High Heat Flux Coke Deposition On Copper Wires

Figure 11, Figure 12, Figure 13, and Figure 14 show data from a test with the 0.015-in diameter copper wire. In Figure 11 we present the fuel flow rates and the pressures measured in the test section. Before the test is started, the pressure in the fuel accumulator was raised to 2235 psig. At 458 seconds the Badger flow control valve was opened and the flow was set to 1 gpm and held for about 30 seconds in order to calibrate the wire resistivity under conditions where the temperature of the wire is near the fuel temperature. At 435 seconds the flow was raised to 3.1 gpm and the flow held relatively stable for the duration of the test, although it dropped to 2.97 gpm just before the end of the test. As shown in the figure, the pressure drop in the reactor resulted in an exit pressure of between 1400 and 1300 psig over the duration of the test. Finally, as noted in the box in the figure, the fuel velocity reached 194 ft/s and the bulk Reynolds number was 46,000 during the test. cooling channels of a rocket engine.

Figure 12 includes the fuel temperatures at the inlet and exit of the test section along with the wire temperature over the length of the test. The wire temperature was calculated in real time during the experiment by using the voltage and current to calculate resistivity and then comparing that value to the known resistivity versus temperature relationship of pure copper[12] (Matula, 1979). The wire temperature reached 566°C at a run time of 500 seconds. After that point, the temperature remained relatively constant over the test duration, dropping only by about 5°C to 561°C by the end of the test. The fuel temperatures entering and exiting the reactor and the differential temperature increased slowly during the test. At a time of 500 seconds, the inlet and exit temperatures were 21.3°C and 33.0°C respectively, while at 550 seconds, the respective values are 21.7°C and 33.9°C. Therefore the differential temperatures were 11.7°C at 500 seconds and 12.2°C at 550 seconds.

The current passing through the wire and corresponding voltages measured during the test are shown in Figure 13. Once steady state conditions were reached, the voltage measured by the power supply was constant at 12.0 V while the value measured across the leads connected to the wire was also constant at 11.7 V. The figure also shows that when the voltage reached 12.0 V,

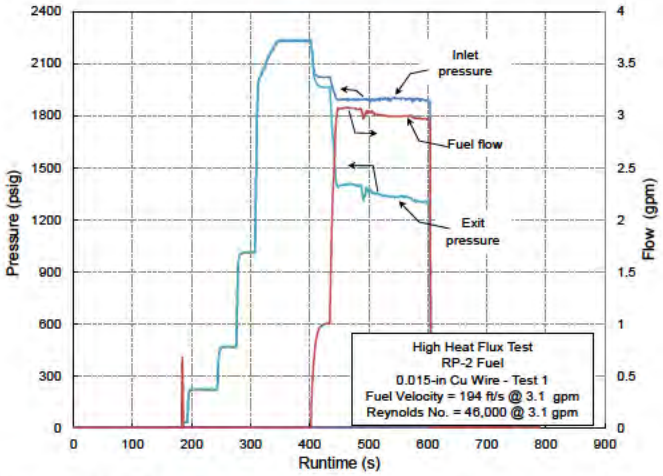

Figure 11. Fuel flow and pressure data during a high heat flux test using RP-2 and a 0.015-in diameter copper wire.

These values are representative of conditions expected in the

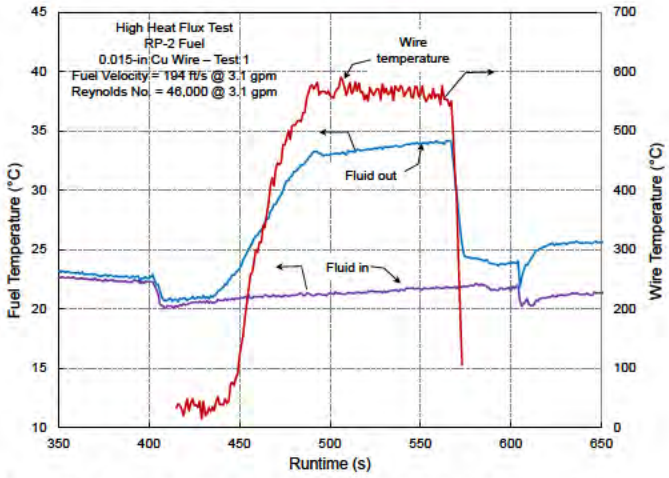

Figure 12. Copper wire temperature along with RP-2 temperatures entering and exiting the test section during the high heat flux test.

the current through the wire was also very stable at 266 amps.

Finally, the heat flux measured during this test is shown in Figure 14. The figure shows that a heat flux of 16.2 Btu/in2-s was reached at a time of 500 seconds and the value was maintained for the duration of the test when the power was stopped at 568 seconds.

We carried out a second high heat flux test with another section of 0.015-in copper wire so that it could be oxidized by our low temperature oxidation process. The conditions reached during this test were very similar to those reported for the previous test and therefore we only included one figure from this test, which shows the heat flux obtained (Figure 15). In this case the heat flux was just under the values we obtained in the previous test. The figure shows that at 294 seconds the heat flux reached 15.6 Btu/in^2-s. After this point, the heat flux remained relatively stable until the power to the test section was shut off at 378 seconds.

Overall the results presented in this section demonstrate that we could expose a pure copper wire test section to heat fluxes of 15-16 Btu/in^2-s, which is very close to the original objective of this project. Higher fuel flow rates were needed to push the heat flux to values of up to 20 Btu/in^2-s, but when the fuel flow was increased over 3 gpm it caused the pure copper wires to break during the test, even up to diameters of 0.020-in (24 gauge). In order to reach higher heat flux values, we needed stronger wires. Results obtained with Copper-Clad Steel (CCS) wires are discussed in the following section.

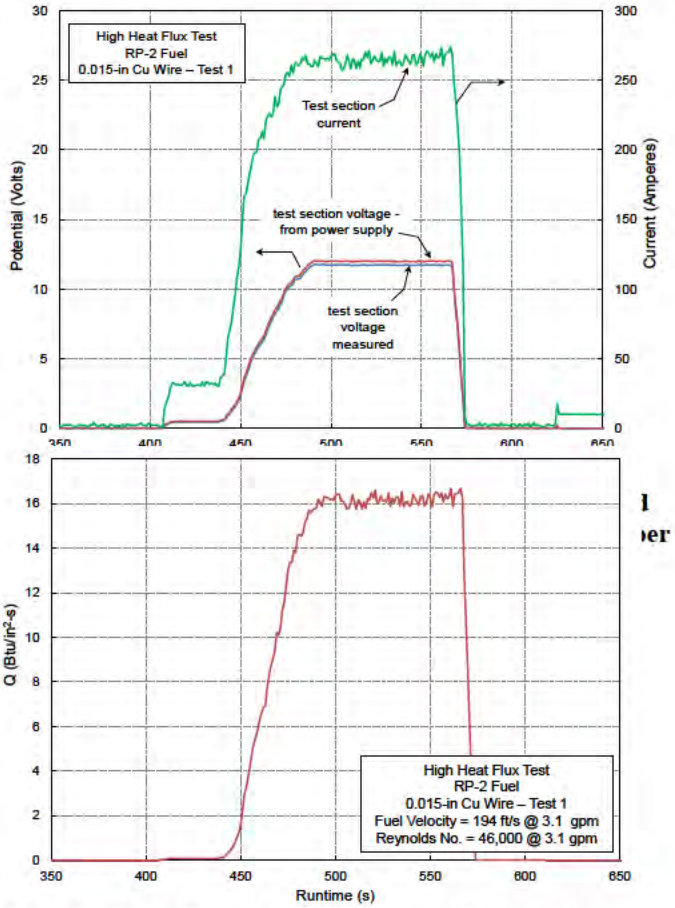

Figure 14. Heat flux data obtained with RP-2 and the 0.015-in diameter copper wire (Test #1).

B. Results of High Heat Flux Coke Deposition with Copper-Clad Steel Wires

In view of the problem with breakage of the copper wires at flow rates below those required, we carried out tests with a composite wire having a pure copper cladding and an inner steel core called Copper-Clad Steel (CCS). This type of wire is commonly used in applications requiring higher strength, such as pulling long runs of cable. We obtained a composite steel and copper wire fabricated by Copperweld Bimetallics, LLC (Fayetteville, TN) that we expected to be strong enough to remain intact at flow rates beyond 3 gallons per minute. We obtained samples of both their annealed 1010 and 1022 steel-cored wire in 24 gauge diameter (0.0201 in) and with an effective overall conductance of 30% of IACS pure copper (International Annealed Copper Standard). Since the conductivity of the underlying steel is approximately 18% IACS, we estimated the thickness of the pure copper layer to be about 0.001 inch. We carried out several tests with the CCS wire and the results obtained are discussed in the following sections.

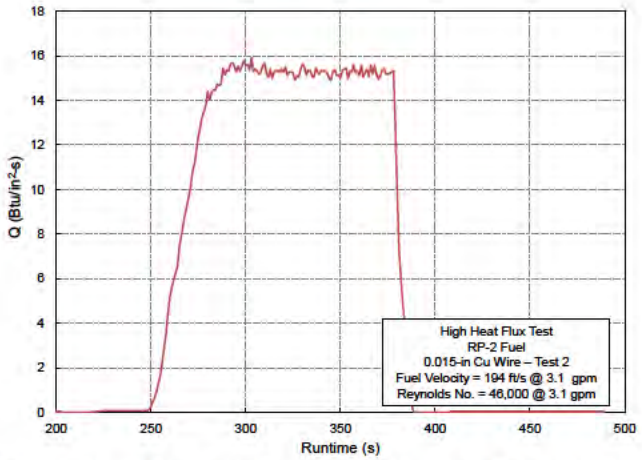

Figure 15. Heat flux data obtained using RP-2 and the 0.015-in diameter copper wire (Test #2).

C. High Heat Flux Test with a 0.020-in Diameter Copper Clad Steel Wire (1022 Carbon Steel Core)

Data from one test with the 1022 alloy CCS wire are shown in Figure 16, Figure 17, Figure 18, and Figure 19. Figure 16 shows the fuel flow rate and the pressures measured in the test section. At 458 seconds the Badger flow control valve was opened and the flow was set to 1 gpm and held for about 30 seconds. During this time a small voltage was applied to the wire to calibrate its resistivity and adjust the temperature correlation so an accurate temperature could be calculated during the rest of the test. At 490 seconds the flow was raised to 3.1 gpm and this flow was maintained for the duration of the test. During this period, the pressure drop in the reactor resulted in an exit pressure of 1440 psig.

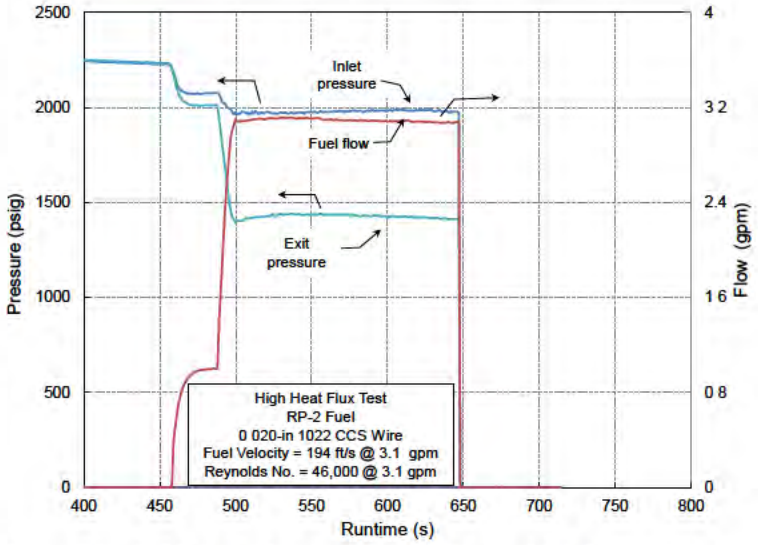

Figure 16. Fuel flow and pressure data during high heat flux test using RP-2 and the 0.020-in, 1022 alloy CCS wire.

Figure 17 includes the wire temperature based on a resistivity versus temperature correlation along with fuel temperatures measured at the inlet and exit of the test section. Since there was no data available on the resistivity versus temperature properties of this wire, the effective resistivity was estimated by assuming that the steel and copper were simply connected in parallel. Electrical resistivity data for annealed low carbon steels were obtained from the Metals Handbook[13] (1978) and a simple multiple linear regression was fit in terms of temperature and the carbon and manganese content of the steel. The average composition of 1022 steel was then used in combination with our previous resistivity fit for pure copper to find the copper cladding thickness that would give us the known overall resistivity of the clad wire at room temperature (30% IACS in this case). The calculated resistivity versus temperature for the separate parallel steel and copper conduction paths was then used to generate new quadratic resistivity fit coefficients to use during the test to estimate the temperature of the wire.

The wire temperature appeared to reach a maximum temperature of 511°C at a run time of 550 seconds. However after that point, the temperature appeared to decrease and, according to the resistivity correlation, dropped to 409°C just before the run was stopped at 640 seconds. The change in fuel temperature exiting the test section is not consistent with the apparent drop in wire temperature, however. At 550 seconds, when the wire temperature was at its maximum, the fuel exit temperature was 35.6°C, 15.5°C greater than the temperature measured at the reactor inlet. However after this point rather than dropping along with the wire temperature, the fuel temperature continued to increase and reached 37.8°C at 581 seconds. At this point, a soft current limit on the power supply was reached and temporarily halted the increase in the fuel temperature. However after this limit was raised at 591 seconds, the fuel temperature

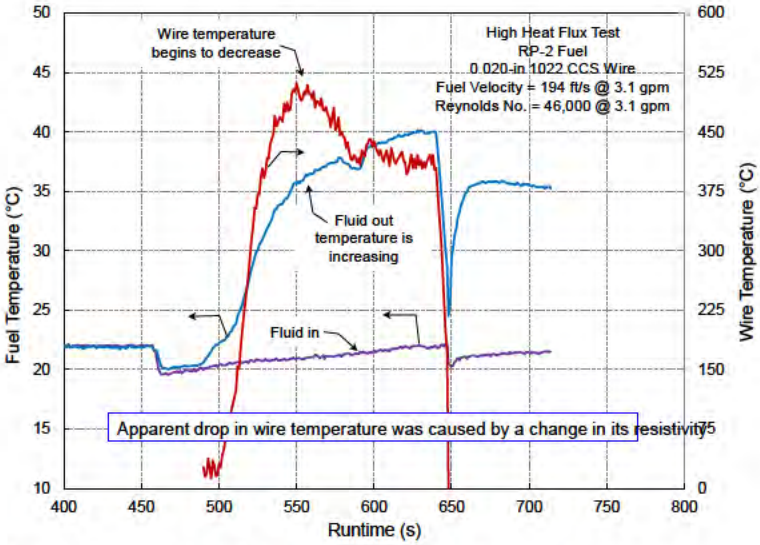

Figure 17. RP-2 and the 0.020-in, 1022 alloy CCS wire temperatures during the high heat flux test.

continued to rise and reached 40°C just before the conclusion of the test, which represents an 18°C temperature rise through the test section. As we will discuss in more detail later, the apparent drop in wire temperature is most likely due to a change in overall resistivity which resulted from a change in the microstructure of the 1022 steel alloy core.

Figure 18 shows the wire current and voltages measured during the test. At 554 seconds, the wire potential (measured across the leads) reached 19.7 V and the measured current was 215 amps. However, at this point, the current continued to increase even though the voltage remained constant. At 581 seconds, the current reached the soft limit, programmed into the power supply which caused the voltage to drop. At 591 seconds the limit was raised, which increased the voltage and caused the current to continue rising, eventually reaching a maximum value of 261 amps just before the test was ended.

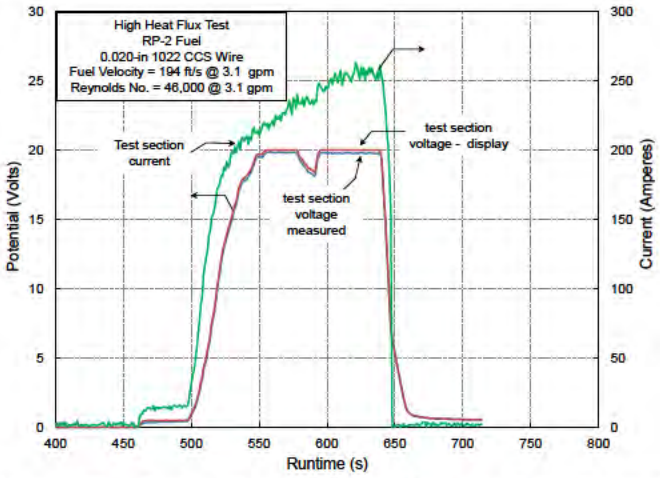

Figure 18. Test section current and voltage data obtained during the test with RP-2 and the 0.020-in, 1022 alloy CCS wire.

The continual increase in current at constant voltage can only be caused by a change in the resistance of the wire test section. Moreover in this set up, the resistance can only be changed by reducing the temperature of the wire or an alteration in the microstructure of the material. As discussed earlier, there is no cause for a drop in wire temperature and it is not consistent with the continual increase in fuel exit temperature. Therefore, we concluded that a change in the crystal structure of the steel occurred when it reached about 500°C and this altered the temperature versus resistivity correlation we used to calculate wire temperature.

The heat flux measured during this test is shown in Figure 19. Unlike the wire temperature, there is no ambiguity in this measurement. Since the heat flux is determined by current, voltage and the surface area of the wire it is not affected by a change in resistance or microstructure of the wire. The figure shows that the heat flux reached a value of 19.8 Btu/in2-s at a runtime of 625 seconds. It then remained close to this value for the next 12 seconds until the test was ended, reaching a maximum heat flux of 20.3 Btu/in2-s during this period. Our original goal was to reach values in the range of 20 Btu/in2-s since this represents the high heat flux levels experienced inside the rocket engine liner cooling channels. Thus, these results show that we achieved this objective.

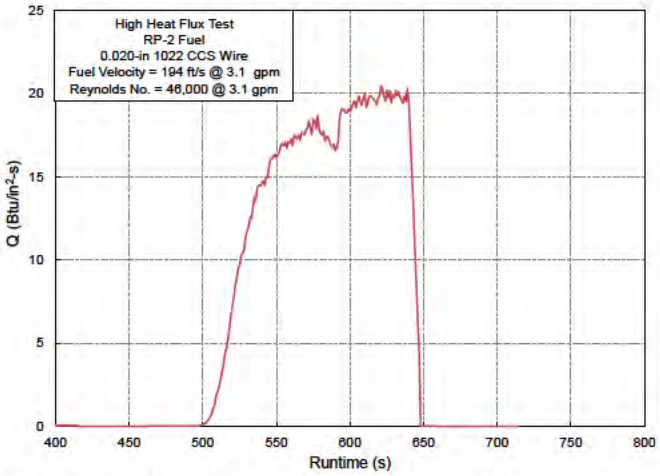

Figure 19. Heat flux data obtained using RP-2 and the 0.020-inch, 1022 alloy CCS wire.

D. High Heat Flux Test with 0.020-in Diameter Copper-Clad Steel (CCS) Wire – 1010 Alloy

We also conducted tests with a CCS wire that contained the 1010 steel alloy, which contains less carbon than the 1022 alloy used in the previous test. In this test we also made two other changes: we incorporated a revised temperature versus resistivity correlation, which we expected to provide a more accurate temperature estimate during the test. We also conducted the test at a somewhat lower heat flux to reduce the extent of any microstructure changes that might occur. We conducted the test at the same nominal flow rate and pressure used in the previous tests, 3.1 gpm and a pressure of 2000 psig at the reactor inlet. The results of this test are shown in Figure 20, Figure 21, and Figure 22.

Distribution A: Approved For Public Release. Unlimited Distribution.

Figure 20 shows the temperatures of the wire along with the fuel (fluid) entering and exiting the test section. In this case the wire temperature reached a maximum value of 566°C at 681 seconds. At the same time, the fluid exiting the reactor was 36.8°C, which was 15.8°C higher than the fuel entering the reactor. Between times of 675 to 700 seconds, the wire temperature remained relatively constant and the fluid exit temperature increased slowly, from 36.7°C to 37.4°C. Although we would not expect the fluid temperature to rise if the wire temperature is remaining constant, the effect is not as significant as it was in Figure 17 where the apparent wire temperature decreased by 50°C at the same time the fuel temperature increased by 2°C. At 707 seconds, the temperatures of the fluid exit and the wire began to decrease. This was caused by the implementation of a current limit in the power supply that reduced the voltage to prevent the current from exceeding 225 amps.

The test section potentials and current are shown in Figure 21. In this test, the potential reached 20 V at 672 seconds and remained constant for the next 36 seconds. During this period, the current increased slowly from 220 to 225 amps. At this point, the limit on the power supply current which was set to 225 amps caused the voltage to drop at a constant rate, eventually reaching 18.6 volts when the test was halted at 737 seconds. The results reported in the last two figures show that although the resistance of this wire also appeared to change, the effect was less significant than observed in the previous test. This could be due to the use of the lower carbon, 1010 alloy, in this CCS wire.

Figure 22 shows the heat flux measured during this test. At 675 seconds, the heat flux reached 17.9 Btu/in2-s. Between 675 and 708 seconds the heat flux increased slowly and reached a maximum of 18.4 Btu/in2-s at 700 seconds. At 708 seconds the current limit reduced the voltage which reduced the heat flux for the last 30 seconds of the test where the heat flux was 16.3 Btu/in^2-s just before the test was stopped at 738 seconds.

E. Heat Transfer Analysis

We used the temperatures of the wire and the change in bulk fuel temperature to calculate a heat transfer coefficient at a number of points during the previous tests and then extracted the corresponding Nusselt number. We also calculated Nusselt Numbers using the Sieder-Tate correlation which relies on characteristics of the fuel flow in the test section. Figure 23

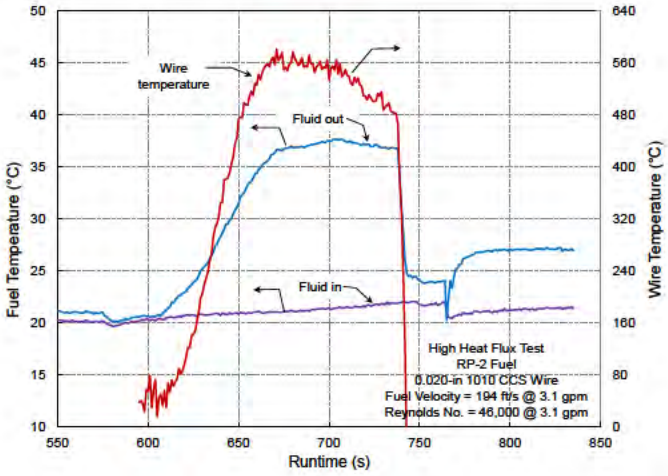

Figure 20. RP-2 and the 0.020-in CCS wire temperatures during the high heat flux test with the 1010 steel alloy.

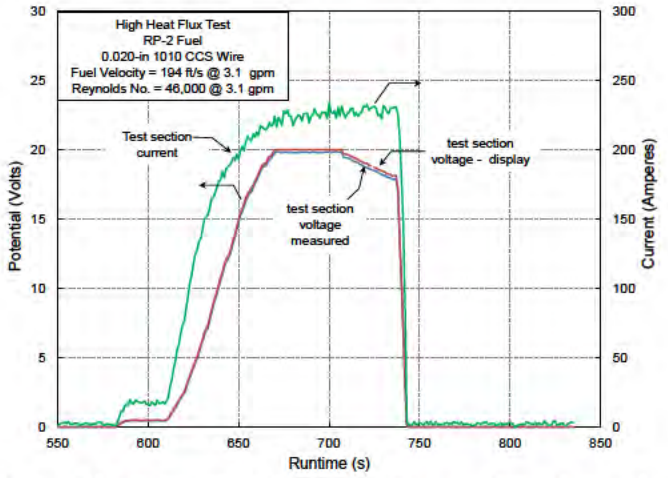

Figure 21. Test section current and voltage data obtained during the test with RP-2 and the 0.020-in 1010 core alloy CCS wire.

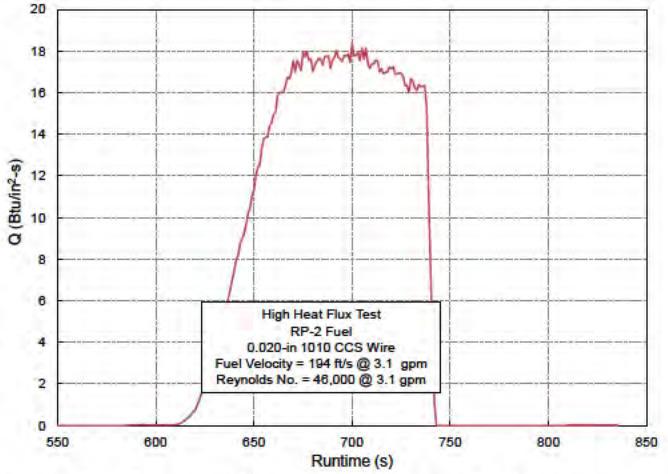

Figure 22. Heat flux data obtained using RP-2 and the 0.020-in, 1010 core alloy CCS wire.

summarizes the results of these calculations for the tests with the 0.015-in copper wire along with the results obtained for the CCS wires. The data for the copper wires including those at the highest Nusselt Numbers agree well with the Sieder-Tate correlation. On the other hand, the numbers for the test with both CCS wires at heat fluxes above about 16 Btu/in^2-s diverged significantly from the correlation. This was caused by using the wire resistivity as to calculate the wire temperature during the test. Since the resistivity changed during the test, it resulted in a calculated temperature that was lower than actual and this in-turn resulted in an overestimation of the fuel-side heat transfer coefficient and Nusselt number. On the other hand, with a pure copper wire, we obtained good agreement between the calculated and measured Nussult Numbers at the highest heat fluxes and therefore have good confidence in the wire temperatures that were measured during the test.

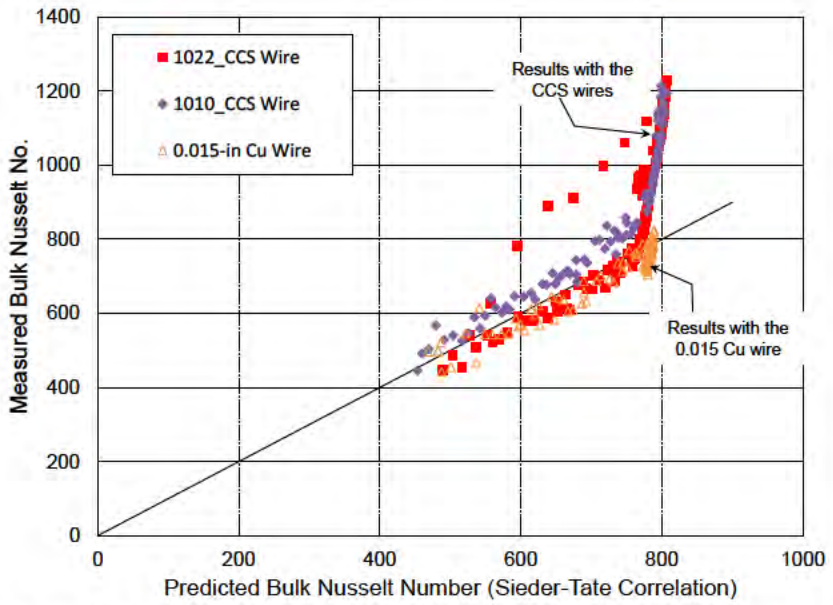

Figure 23. Measured Nusselt Numbers plotted against values calculated using the Sieder-Tate Correlation.

As mentioned previously, we believe that the decrease in the wire resistivity is due to microstructural changes in the steel that occur at temperatures above 500°C, but still well below the well-known alpha to gamma (mixed ferrite+cementite [iron carbide] to austenite) iron phase transition that occurs at 1333°F (723°C) as shown in Figure 24. Specifically, this decrease in wire resistivity is probably due to dissolving previously precipitated iron carbide back into the ferrite matrix, improving the electrical conductivity of the steel. Only about an 8% change in steel conductivity is required to explain the anomalously low indicated wire temperatures observed in this test at the highest heat flux. Using the measured heat flux and the Sieder-Tate correlation as the basis of the predicted wire surface temperature, we estimate that we actually achieved a wire temperature near 600°C at the highest heat flux condition. The last seven data points collected during this run (proceeding down and to the left from the peak) indicate that the wire resistivity was starting to approach nominal values again during the current/voltage rampdown as the temperature of the wire decreased.

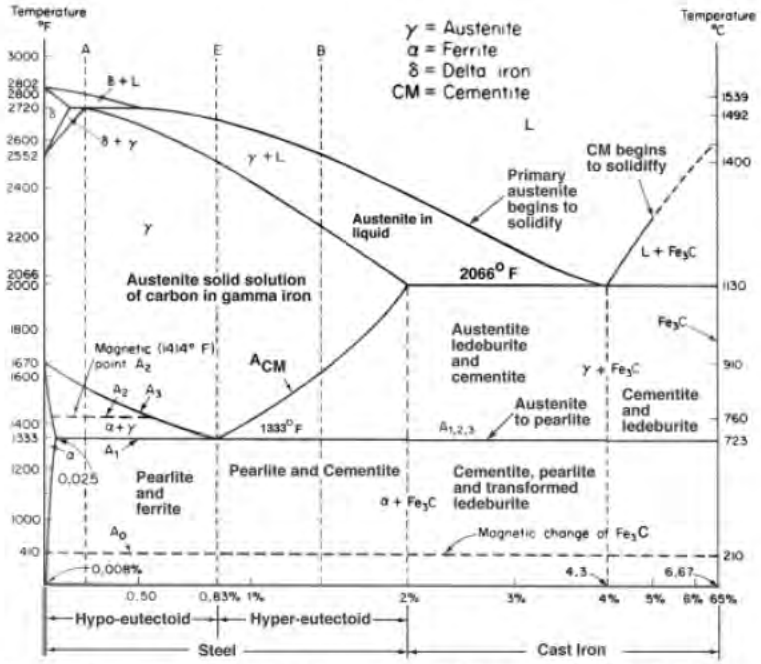

Figure 24. Fe-Fe_3C equilibrium phase diagram (from Pollack[14], 1988).

F. Surface Characterization of Copper Wires by AES

One of the benefits of the test section we designed in this project is the ability to remove the test wire and carry out surface analysis on it directly without additional preparation. On the other

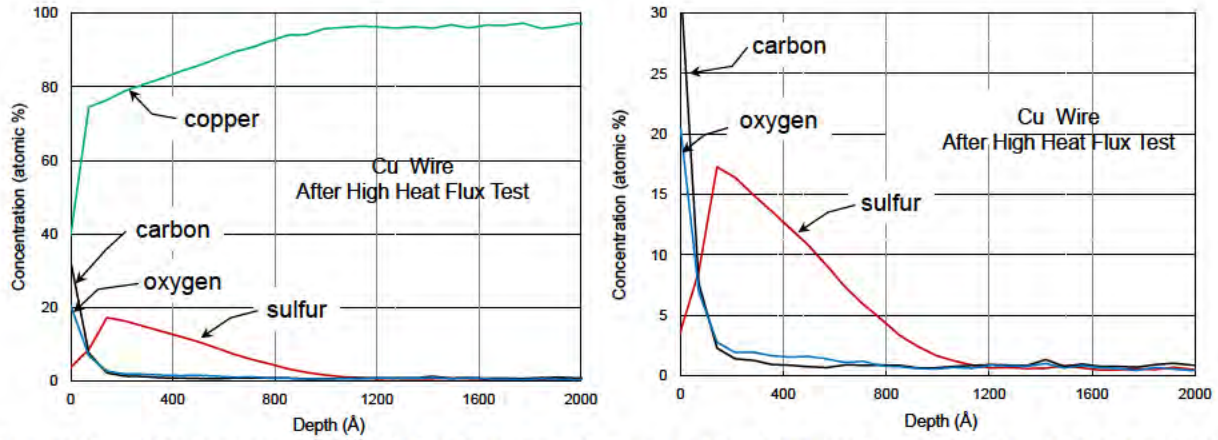

Figure 25. AES analyses of the 0.015-in Cu wire after one test at high heat flux: left side - full scale, right side – expanded Y axis.

hand, when tests are conducted inside a small tube, it must be cut open to expose the coked surface. Such harsh treatment can affect the coke or sulfur layers that have accumulated on the inner surface or introduce contamination and produce inaccurate or misleading results.

After the coke deposition testing was complete on all four wire samples, we exposed one copper and one CCS wire to our low temperature oxidation process. We then submitted all four samples for surface analysis by Auger Electron Spectroscopy (AES). AES characterize the concentrations of elements, including carbon and sulfur, as a function of depth in the outer atomic layers of the sample. Results obtained on the two samples analyzed after the coking process are expected to simulate the surface composition of the copper in the cooling channels of a rocket engine. On the other hand, results obtained on samples that were exposed to the coking conditions followed by the low temperature oxidation process are representative of rocket engine cooling channels after being treated to remove coke. The AES results obtained for the coked 0.015-in diameter Cu wire are shown in Figure 25. The figure on the left side shows that the copper concentration is about 40% at the surface and the rest of the surface is comprised primarily of carbon and oxygen. The carbon concentration is approximately 35% at the surface. The plot with the expanded axes (on the right side of Figure 25) shows that the carbon concentration decreases rapidly with depth and is less than 4% at a depth of 200 Å, which is about 0.8 millionths of an inch. Thus, these results show indicate that exposing copper to a heat flux of 16 Btu/in^2-s for a period of two minutes can result in a significant accumulation of carbon on the surface. Finally, the figure also shows that a measurable quantity of sulfur has accumulated. At the surface the concentration is about 4% but, surprisingly, it increases with depth and reaches a value of about 17% at a depth of about 200 Å. The sulfur concentration then decreases to less than 5% at a depth of approximately 1000 Å.

We then used our low temperature process with O_3 to oxidize one of the copper wires after it had been exposed to high heat flux conditions and had AES analyses carried out on it. The results of these analyses are shown in Figure 26. The figure shows that the surface is comprised of O and Cu in roughly equal concentrations and indicates that the low temperature oxidation process has been extremely effective in oxidizing all of the carbon that had accumulated on the

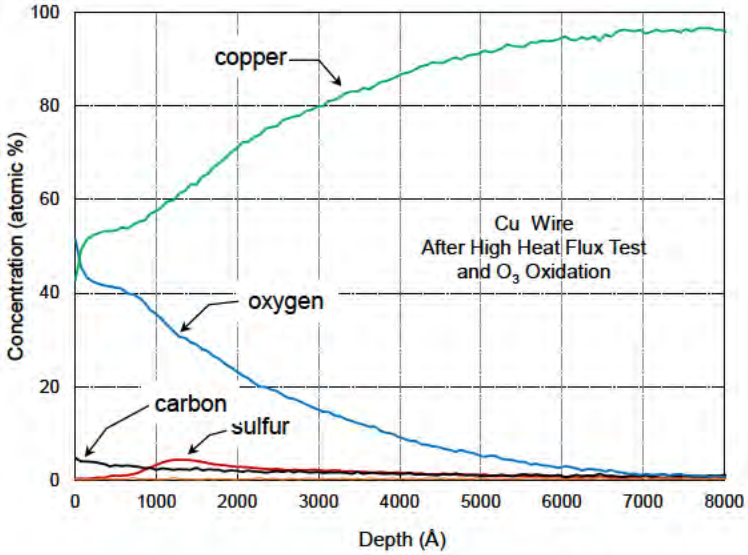

Figure 26. AES analyses of the 0.015-in diameter Cu wire after the test at high heat flux and low temperature oxidation with O_3.

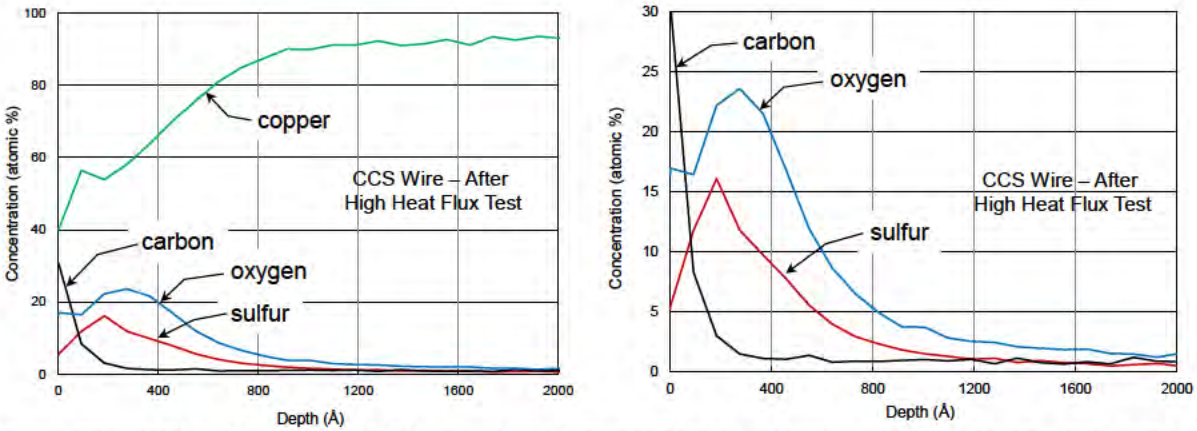

Figure 27. AES analyses of the CCS wire after the test at high heat flux conditions: left side - full scale, right side – expanded axes.

wire surface. At a depth of less than a millionth of an inch, the thermal resistance would not have caused a substantial issue. However if the rocket engine was to be reused, then similar carbon accumulations could be expected during each mission, and this could ultimately lead to a failure in the heat exchanger. However, if the low temperature oxidation process were applied between missions, then dangerous levels of coke accumulation could be prevented.

G. Surface Characterization of the CCS Wires by AES

The results obtained for the CCS samples are included in Figure 27 and Figure 28. Figure 27 shows an AES depth profile on the CCS wire after it was exposed to high heat flux conditions. The figure on the left side shows that at the surface, the composition is about 40% Cu and that carbon, oxygen, and sulfur comprise the balance of the surface. The data presented on expanded X and Y axes show that the surface concentrations of carbon, oxygen and sulfur are 30%, 16% and 6% respectively. The carbon concentration decreases rapidly and is less than 5% at a depth of 300 Å or 30 nm. This represents a carbon thickness of just over 1 millionth of an inch, similar to results obtained on the pure copper wire. Once again, the wire also contains a substantial layer of sulfur. The concentration is low at the surface, reaches a maximum of 16% at a depth of approximately 250 Å, and then declines to less than 5% at a depth of 1000 Å or four millionths of an inch.

The results obtained on the CCS wire after oxidation are included in Figure 28. The figure shows that the only two elements at the surface of the wire are copper and oxygen. These results show that the low temperature oxidation process was very effective at removing the carbon deposited on the surface. In addition, similar to the results obtained on the coper wire, the figure also shows the oxidation process has removed the sulfur layers that had been deposited on the wire surface. Finally, the figures shows that the oxygen layer penetrates deeply into the copper metal, to about 1.5 µm, which is much deeper than the oxide layer reached for the copper wire. The temperature reached during the oxidation of the CCS wire was approximately 170°C while the temperature reached with the Cu wire was somewhat lower, at 140°C. Therefore we conclude that the thinner oxygen layer obtained in the test with the copper wire is due to the lower temperature reached during the oxidation process. It is likely that the carbon deposits can be removed at lower temperatures which will leave a thinner layer of oxygen in the outer layers of the copper surface.

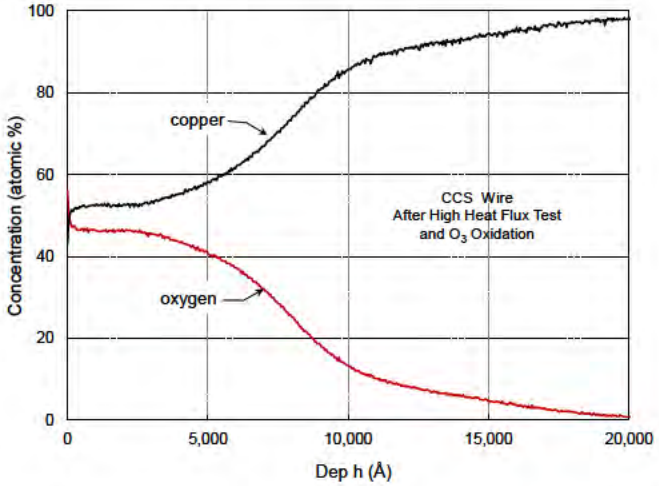

Figure 28. AES analyses of the CCS wire after the test at high heat flux and low temperature oxidation with O_3.

H. Surface Analysis After Three Coking/Oxidation Cycles

We carried out a series of tests on one 0.015-in diameter copper wire test section in which we exposed the wire to three cycles of coking followed by low temperature oxidation. In the coking tests, we reduced the fuel flow rate to prevent the wire from breaking but obtained temperatures in the range where coke deposition would be expected. In Figure 29 we have combined the temperatures obtained for the three coking cycles. The figure shows that in all tests similar temperatures were obtained. We also obtained very similar test conditions during the oxidation steps performed after each coke deposition test. These results demonstrate that we have achieved good control of the important experimental parameters in these tests and therefore we conclude that the surface data we obtain following these coke deposition and oxidation cycles should accurately reflect the surface composition of the copper surfaces in the cooling channels of a liquid fueled rocked engine.

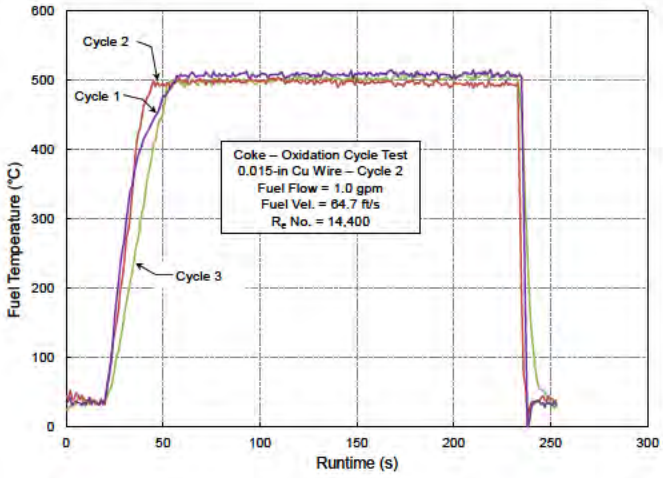

Figure 29. Combined wire temperatures measured during the three cycling tests with the 0.015-in diameter copper wire.

As pointed out above, these tests were carried out at lower fuel flow rates in order to maximize the cycle time of the wire test section. Despite reducing the flow, the 0.015-in OD wire broke after three coking and oxidation cycles. We then started cycling a second wire that was 0.020-in in diameter and this wire broke after 2 and ½ cycles. In both cases, we had difficulty removing and installing the wire in the coke deposition rig which contributed to the weakening of the wire and its subsequent failure, presumably through low-cycle fatigue. We then disassembled the test section housing and found that the bottom housing had become bent. This section was straightened, which improved the ease of wire installation and removal steps. Unfortunately, this wire also broke after three cycles. A subsequent review of the literature suggests that high current densities flowing through the wire can also cause it to weaken through a process called electromigration[15].

After the third full cycle on the wire, it was submitted for AES analysis. The results are shown in Figure 30. Two conclusions can be drawn from the figure. First, the figure shows that the concentration of carbon at the surface is much lower than after a single coking cycle and therefore the data indicate that the oxidation process is effective. At the surface the carbon concentration is approximately 15% and it drops rapidly, in less than 100 Å or 10 nm, to less than 5%. By contrast, data included in Figure 25 and Figure 27 show that after a single coking cycle at high temperatures, the carbon concentration is on the order of 30%.

Although the cycle data indicate that coke can be controlled by oxidation after each coking cycle, the data in Figure 30 show that the concentration of sulfur in the copper metal increased over the three tests. At a depth 500 Å, the sulfur concentration is 20% and is greater than 10% between depths of 200 Å and 2500 Å. On the other hand, the data in Figure 26 show that after a single coke and oxidation cycle carried out under identical conditions, the sulfur concentration is approximately 5%. Once again these tests were done with RP-2 fuel so we conclude that sulfur at even very low levels will react with copper under high

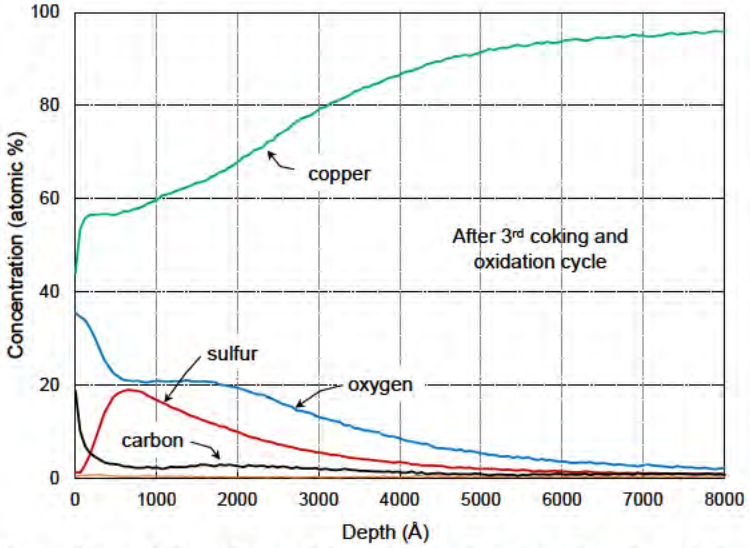

Figure 30. AES analyses of the 0.015-in Cu wire after three full coking and oxidation cycles.

heat flux conditions to produce a form of copper sulfide.

I. Sulfur accumulation with RP-2 Fuel

The presence of sulfur on the wire samples was surprising because the sulfur content in the fuel met the RP-2 specification of less than 100 ppb. We had several fuel samples that had been extracted over the course of the test campaign analyzed for sulfur, including a sample directly out of the supply barrel. We also charged our fuel accumulator with RP-2 without running a high heat flux test then removed a small portion for analysis. The results of these analyses are shown in Table 1, and in all cases the results are below the RP-2 specification of 0.1 ppm. Therefore, our surface analysis data show that sulfur will accumulate on the walls of rocket engine cooling channels if they are reused, which could potentially lead to problems over the course of several missions. Our coke oxidation process appears to also be able to remove sulfur if it is conducted at a high enough temperature, however this leaves a rather thick oxygen layer behind on the surface of the copper. The development of a fuel additive to block the surface reaction of sulfur with copper could therefore be an enabling technology for reusable rocket engines.

Table 1. Results of sulfur analyses.

Sample	(ppm)
RP-2 – out of the barrel	0.04
RP-2 Fuel accumulator before tests	0.09
RP-2 Reservoir after test	0.08

V. Summary and Conclusions

In this project we developed a test section that had the capability of exposing a copper test section to heat fluxes up to 20 Btu/in^2-s, which are representative of those expected in the cooling channels of a liquid fueled rocket engine. Moreover, the results indicated that exposure to such conditions for periods of less than three minutes results in the deposition of coke layers that are on the order of 0.5 millionths of an inch thick. Although these thicknesses would not be expected to cause a failure in the heat exchanger, similar accumulations over the course of multiple missions could results in a substantial reduction in thermal conductivity and heat exchanger failure. In addition, the test results showed that sulfur build up even with RP-2 grade fuel could potentially become a concern. However, the test data also show that our low temperature oxidation process is effective at removing both coke and sulfur. Thus, such a treatment between missions could eliminate hazards associated with carbon or sulfur build up over multiple engine missions.

VI. Acknowledgements

The authors gratefully acknowledge funding for this work which was provided under SBIR Contract No. FA9300-13-C-2012. We would also like to thank our contract monitor, Capt. Diane Fernandes for her thoughtful comments over the course of this project and for providing the RP-2 that was used in our experimental work.

Distribution A: Approved For Public Release. Unlimited Distribution.

VII. References

[1]Edwards, J.T. (2003). "Liquid Fuels and Propellants for Aerospace Propulsion: 1903-2003," *Journal of Propulsion and Power*, **19**(6):1089-1107.

[2]Huzel, D. K. and Huang, D.H. (1992). *"Modern Engineering for Design of Liquid-Propellant Rocket Engines,"* American Institute of Aeronautics and Astronautics, Washington, DC.

[3]Hazlett, R.N. (1991). "*Oxidation Stability of Aviation Turbine Fuels,"* ASTM, Philadelphia, PA.

[4]Wickham, D.T., J.R. Engel, and B.D. Hitch (2013). *"A Novel Method for Rapid Coke Measurement in Liquid Rocket Engines,"* JANNAF 2013-3242, 29 April – 3 May, Colorado Springs, CO.

[5]Roback, R., Szetela, E.J., and Spadaccini, L.J. (1981). *"Deposit Formation in Hydrocarbon Rocket Fuels,"* NASA Contractor Report 165405. Accessed at: http://ntrs nasa.gov/archive/nasa/casi ntrs.nasa.gov/19810021741.pdf

[6]Rosenburg, S.D. and Gage, M.L. (1991). "Compatibility of Hydrocarbon Fuels with Booster Engine Combustion Chamber Liners," *J. of Propulsion and Power* **7**(6):922-928.

[7]Billingsley, M.C. (2008). *"Thermal Stability and Heat Transfer Characteristics of RP-2,"* Paper No. AIAA 2008-5126, presented at the 44th AIAA/ASME/SAE/ASEE Joint Propulsion Conf., Hartford CT.

[8]Van Noord, J.L. and Stiegemeir, *"RP-2 Thermal Stability and Heat Transfer Investigation for Hydrocarbon Boost Engines"*, 57th JANNAF 2010-216917, 3-7 May, 2010, Colorado Springs, CO.

[9]Kleinhenz, J., Deans, M., Stiegemeier, B., and Psaras, P. (2013). *"Thermal Stability of RP-2 for Hydrocarbon Boost Regenerative Cooling,"* presented at the 60th JANNAF Propulsion Meeting; 29 Apr. - 3 May, Colorado Springs, CO.

[10]Billingsley, M.C. H.Y. Lyu and R.W. Bates (2007). *"Experimental and Numerical Investigations of RP-2 Under High Heat Fluxes,"* Presented at the JANNAF 54th Propulsion Meeting/3rd Liquid Propulsion Subcommittee/2nd Spacecraft Propulsion Subcommittee/5th Modeling and Simulation Subcommittee Joint Meeting, Denver, CO, 14-17 May.

[11]Linne, D.L., M. L. Meyer, T. Edwards, and D. A. Eitman (1997). *"Evaluation of Heat Transfer and Thermal Stability of Supercritical JP-7 Fuel,"* Paper No. 33rd AIAA, ASME, SAE, and ASEE Joint Propulsion Conference and Exhibit, July 6–9, Seattle, WA.

[12]Matula, R.A. (1979). "Electrical Resistivity of Copper, Gold, Palladium, and Silver," *J. Phys. Chem. Ref. Data* **8**(4):1147-1298.

[13]Metals Handbook (1978). *"Volume 1 - Properties and Selection: Irons and Steels,"* 9th ed., pg. 151, American Society for Metals, Metals Park, OH.

[14]Pollack, H.W. (1988). *"Materials Science and Metallurgy,"* 4th ed., Prentice-Hall, Upper Saddle River, NJ.

[15]Lienig, J. (2006). *"Introduction to Electromigration-Aware Physical Design,"* presented at the ACM International Symposium on Physical Design, , 9 – 12 April, San Jose CA. Accessed at: http://www.ifte.de/mitarbeiter/lienig/ispd06_emPaper_lienig.pdf

Distribution A: Approved For Public Release. Unlimited Distribution.